DEVELOPMENT OF THIN FILMS DEPOSITED BY ALD FOR c-SI SOLAR CELLS

A Degree Thesis
Submitted to the Faculty of the
Escola Tècnica d'Enginyeria de Telecomunicació de Barcelona
Universitat Politècnica de Catalunya
by
Javier Pérez Guardia

In partial fulfilment
of the requirements for the degree in
ELECTRONIC ENGINEERING

Advisor: Isidro Martín García

Barcelona, January 2017

Abstract

In this work, we have developed thin layers deposited by Atomic Layer Deposition (ALD) technique to be applied in high-efficiency crystalline silicon solar cells. In particular, we selected to study the aluminium oxide (Al_2O_3) as a surface passivation mechanism and the titanium dioxide (TiO_2) as a selective contact for electrons.

To characterize the Al_2O_3 we have done two studies: deposition thickness and pre-deposition cleaning process. In both studies we have measured the effective surface recombination velocity (S_{eff}), where we get results comparable to the state of the art with $S_{eff} < 10$ cm/s. In addition, we demonstrate that less aggressive cleanings of the silicon surface before layer deposition lead to similar results.

On the other hand, to characterize the TiO_2, we have studied the S_{eff} depending on the deposited film thickness and also depending on the deposition temperature. For the 0.6 nm layer we get a specific contact resistance below 100 $m\Omega \cdot cm^2$. This results together with a S_{eff} value in the 100 cm/s demonstrates that this layer is a promising candidate to be used in the development of high-efficiency solar cells.

Resum

En aquest treball hem desenvolupat fines capes, dipositades usant la tècnica de la ALD (Atomic Layer Deposition), per aplicar-les a cèl·lules solars de silici cristal·lí d'alta eficiència. Per fer l'estudi hem seleccionat l'òxid d'alumini (Al_2O_3), més conegut com a alúmina, per usar-ho com a mecanisme de passivació de la superfície, i el diòxid de titani (TiO_2) com a contacte selectiu d'electrons.

Per a la caracterització de l'alúmina hem realitzat dos estudis: grossor de la deposició i procés de neteja previ a la deposició. En tots dos casos hem mesurat la velocitat efectiva de recombinació a la superfície (S_{eff}), en els quals vam obtenir resultats semblants als de l'apartat 2 d'aquest document, amb una $S_{eff} < 10$ cm/s. A més, hem demostrat que amb neteges menys agressives obtenim valors molt semblants als que s'obtenen amb un procés de neteja normal.

Per altra banda, per caracteritzar el diòxid de titani, hem estudiat la S_{eff} depenent del grossor de la capa depositada i en funció de la temperatura de dipòsit. Per a la mostra de 0,6 nm de grossor hem obtingut una resistència de contacte específica per sota de 100 m$\Omega \cdot$cm^2. Això, juntament amb una S_{eff} de 100 cm/s, demostra que aquesta capa és una capa prometedora per utilitzar-se en el desenvolupament de cèl·lules solars d'alta eficiència.

Resumen

En este trabajo hemos desarrollado finas capas, depositadas mediante la técnica ALD (Atomic Layer Deposition), para aplicarlas en células solares de silicio cristalino de alta eficiencia. En particular, hemos elegido para el estudio óxido de aluminio (Al_2O_3), más conocido como alúmina, para usarlo como mecanismo de pasivación de la superficie, y dióxido de titanio (TiO_2) como contacto selectivo para electrones.

Para la caracterización de la alúmina hemos realizado dos estudios: grosor de deposición y proceso de limpieza pre-deposición. En ambos casos hemos medido la velocidad efectiva de recombinación en la superficie (S_{eff}), donde obtuvimos resultados parecidos a los mencionados en el apartado 2 de este documento, con $S_{eff} < 10$ cm/s. Además, hemos demostrado que con limpiezas menos agresivas, obtenemos valores muy similares a los que se obtienen con un proceso de limpieza estándar.

Por otra parte, para caracterizar el dióxido de titanio, hemos estudiado la S_{eff} en función del grosor de la capa depositada y en función de la temperatura de deposición. Para la muestra de 0,6 nm de grosor hemos obtenido una resistencia de contacto específica por debajo 100 m$\Omega \cdot$cm^2. Esto, junto con una S_{eff} de 100 cm/s, demuestra que esta capa es una candidata prometedora para ser usada en el desarrollo de células solares de alta eficiencia.

Acknowledgements

First of all, I would like to express my gratitude to my project tutor Isidro Martín for being always available to help me in some steps of the project, and for teaching me a lot of interesting things about this topic.

I would also like to thank to professor Pablo Ortega and to PhD students Gema López and Gerard Masmitjà who teach me all the necessary processes to carry out my project. Without their help I could not have done my work.

Revision history and approval record

Revision	Date	Purpose
0	27/12/2016	Document creation
1	10/01/2017	Document revision
2	12/01/2017	Document revision
3	13/01/2017	Document revision
4	14/01/2017	Final version

DOCUMENT DISTRIBUTION LIST

Name	e-mail
Javier Pérez Guardia	javier.perez.guardia@gmail.com
Isidro Martín García	Isidro.martin@upc.edu

Written by:		Reviewed and approved by:	
Date	27/12/2016	Date	14/01/2017
Name	Javier Pérez Guardia	Name	Isidro Martín García
Position	Project Author	Position	Project Supervisor

Table of contents

The table of contents must be detailed. Each chapter and main section in the thesis must be listed in the "Table of Contents" and each must be given a page number for the location of a particular text.

List of Figures

List of Tables

1. <u>Introduction</u>

1.1. <u>Project background</u>

The idea emerged because of the necessity to characterize aluminium oxide (Al_2O_3) layers deposited by a new Atomic Layer Deposition (ALD) system recently acquired by the MNT group. In addition, we want to develop new recipes for the deposition of Titanium Dioxide (TiO_2). Both films are to be applied to crystalline silicon (c-Si) solar cells. Obviously, the initial idea was provided by the supervisor of this project and this project is not a continuation of any previous project.

The project is performed at the UPC's Electronic Engineering. The c-Si samples are provided by the Micro and Nano Technologies (MNT) group. Although the new ALD tool has recently been acquired, researchers have been working with a similar tool for many years at ICFO (Instituto de Ciencias Fotónicas). As a consequence, the researchers in the group have acquired a solid knowledge in the process, especially in the Al_2O_3 deposition. This knowledge will be a useful base to develop the project.

Consequently, the purpose of this project is double. On one hand we would like to reproduce passivation results that up to now have been obtained in external laboratories using Al_2O_3 films. In this case the main characteristic to study is the recombination velocity. On the other hand we want to develop an electron transport layer using TiO_2 films, based on the literature. In this case, apart from surface passivation, we would like to study the contact resistance. Also, for all the samples we want do other characterization techniques measurements like ellipsometry to know the thickness of the deposited layers.

1.2. <u>Goals</u>

The main goals of the project can be divided in two parts, one for aluminium oxide (Al_2O_3) and the other one for the titanium oxide (TiO_2).

For the aluminium oxide, the target is to study the behaviour of the surface passivation depending on the deposited layer thickness, and also depending on the previous cleaning process.

And for the titanium oxide, the goals are to study the surface passivation and the contact resistance depending on the thickness, and then study the same variables changing the deposition temperature.

1.3. <u>Work plan packages, milestones and Gantt diagram</u>

1.3.1. Work packages

Project: Documentation	WP ref: WP1	
Major constituent: Reports	Sheet 1 of 4	
Short description: Writing reports the summarize the obtained results and help in the project management	Planned start date: 26/09/2016 Planned end date: 10/01/2017	
	Start event: Project beginning End event: Project end	
Internal task T1: Project proposal and workplan Internal task T2: Project critical review Internal task T3: Final report	Deliverables: D1.1 Project proposal D1.2 Project critical review D1.3 Project final report	Dates: 10/10/2016 20/11/2016 10/01/2017

Table 1.1: WP1

Project: Al_2O_3 (Aluminium Oxide)	WP ref: WP2	
Major constituent: Deposition of the dielectric	Sheet 2 of 4	
Short description: Deposition of Al_2O_3 changing the thickness and the preliminary cleaning process.	Planned start date: 19/09/2016 Planned end date: 21/11/2016	
	Start event: Project beginning End event: Al_2O_3 characterization end	
Internal task T1: Changes on the thickness Internal task T2: Changes on the cleaning process	Deliverables: D2.1 Documentation of Al_2O_3 processes	Dates: 21/11/2016

Table 1.2: WP2

Project: TiO$_2$ (Titanium dioxide)	WP ref: WP3
Major constituent: Deposition of the dielectric	Sheet 3 of 4
Short description: Deposition of TiO$_2$ changing the thickness and the deposit temperature.	Planned start date: 25/10/2016 Planned end date: 19/12/2016
	Start event: Al$_2$O$_3$ depositions end End event: TiO$_2$ characterization end

Internal task T1: Changes on the thickness Internal task T2: Changes on the deposit temperature	Deliverables: D3.1 Documentation of TiO$_2$ processes	Dates: 19/12/2016

Table 1.3: WP3

Project: Characterization	WP ref: WP4
Major constituent: Implementation and assembly	Sheet 4 of 4
Short description: Characterization of the passivation, ellipsometry, I/V* curves and XRD*. *Only for TiO$_2$	Planned start date: 19/09/2016 Planned end date: 23/12/2016
	Start event: Project beginning End event: TiO$_2$ characterization end

Internal task T1: Characterization of Al$_2$O$_3$ samples Internal task T2: Characterization of TiO$_2$ samples Internal task T3: Comparison of characteristics	Deliverables: D4.1 Table of characteristics of the Al$_2$O$_3$ samples D4.2 Table of characteristics of the TiO$_2$ samples D4.3 Comparison of characteristics for each dielectric material.	Dates 25/10/2016 06/12/2016 23/12/2016

Table 1.4: WP4

1.3.2. Milestones

WP#	Task#	Short title	Milestone / deliverable	Date (week)
1	1	Project proposal and workplan	D1.1	10/10/2016
1	2	Project critical review	D1.2	20/11/2016
1	3	Final report	D1.3	10/01/2017
2	1	Al_2O_3 film with surface recombination velocity below 10 cm/s and less than 15 nm	M2.1	24/10/2016
2	1	Documentation of Al_2O_3 processes	D2.1	21/11/2016
3	1	TiO_2 film with specific contact resistance below 100 m$\Omega\cdot$cm^2 and surface recombination velocity below 150 cm/s	M3.1	07/11/2016
3	2	Documentation of TiO_2 processes	D3.1	19/12/2016
4	1	Table of characteristics of the Al_2O_3 samples (S_{eff}, thickness)	D4.1	25/10/2016
4	2	Table of characteristics of the TiO_2 samples (S_{eff}, contact resistance,	D4.2	06/12/2016
4	3	Complete comparison of characteristics depending on changes for each dielectric material	D4.3	23/12/2016

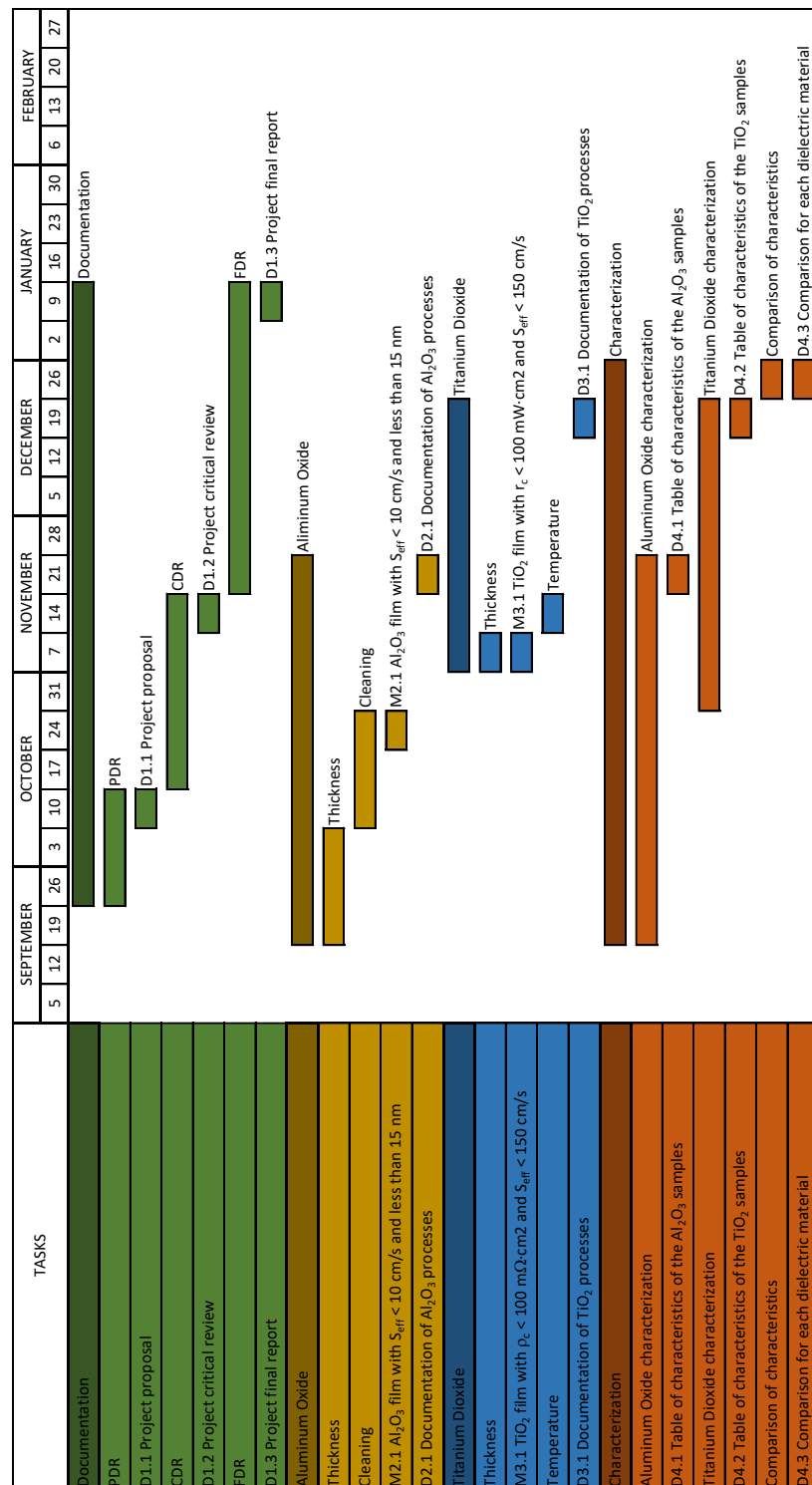*Table 1.5: Milestones*

1.3.3. Gantt diagram

Figure 1.1: Gantt

2.   State of the art

The state of the art of this project is an introduction to the physics of Al_2O_3 c-Si surface passivation and TiO_2 selective contacts.

2.1. Al_2O_3 surface passivation

There are two ways to reduce the recombination losses at a semiconductor interface. The first one is to reduce the number of defect states at the interface because the recombination rate is directly proportional to the interface defect density. We can significantly reduce the interface defect density using a thin dielectric or semiconductor film that covers the dangling bonds at the end of the crystal lattice. This strategy is usually referred as chemical passivation.

The other strategy is called field-effect passivation. The physics that involves this strategy is the reduction of the electron or hole concentration at the semiconductor interface. The recombination processes require both electrons and holes, then the highest recombination rate is obtained when the electron and hole concentration at the interface are approximately equal in magnitude. If the concentration of electron and hole is not equal in magnitude, the recombination rate scales with the lowest carrier concentration at the surface whose availability is limiting the recombination processes. The way to unbalance the electron-hole concentration at the surface is by putting a doping profile below the interface, increasing the concentration of only one type of carriers, or having the presence of fixed electrical charges at semiconductor interface. In the second case, the electric field at the interface makes possible that an electrostatic shielding of the charge carriers alters the electron or hole concentration at the semiconductor interface.

Al_2O_3 passivates the surface in the two ways explained before. Firstly, a density of states in the range of 10^{11} $cm^{-2}eV^{-1}$ is obtained at the c-Si/Al_2O_3 interface which can be considered as relatively low ([1] and references there in). In addition, this material at Al_2O_3/Si surface has a high fixed negative charge density (Q_f) in the range of 10^{12}-10^{13} cm^{-2} which means that produces an effective field-effect passivation by shielding electrons from the interface as explained before [1]. Typically, a post-deposition annealing at 400 ºC for some minutes is needed to get such high values of fixed charge densities simultaneously with a significant reduction of the interface defect density [1]. Several groups are working in the deposition of Al_2O_3 by ALD applied to c-Si solar cells. Some examples are included in table 2.1.

Negative Q_f (cm^{-2})	D_{it} ($eV^{-1}cm^{-2}$)	Deposition method	Deposition temperature (ºC)	Postdeposition thermal treatment	Reference
0.6×10^{12}	$\sim 1 \times 10^{11}$	ALD from $Al(CH_3)$+H_2O	450	None	[2]
$\sim 2 \times 10^{12}$	0.8×10^{11}	ALD from $Al(CH_3)$+H_2O	350	Various at 585 °C and 800 °C	[3]
6×10^{12} – 7×10^{12}	1×10^{11}	ALD from $Al(CH_3)$+H_2O	350	Anneal in N_2 at 450 °C	[4]

Table 2.1: Al_2O_3 deposit examples

In addition, the MNT research group at Universitat Politècnica de Catalunya (UPC) has been working with Al_2O_3 films in the last years with excellent results in their application to solar cells [5-7]

2.2. TiO$_2$ as a selective contact

A selective contact works as a contact where only one type of carriers can flow through. Using one electron and one hole selective contact in a solar cell, photogenerated charge carriers can be collected in separated contacts creating an operational current in the external circuit.

TiO_2 is an interesting candidate to make passivated selective contacts for electrons because it has a small conduction-band offset and a large valence-band offset when is in contact with crystalline silicon. This behaviour is interesting to develop the electron contact for c-Si high-efficiency solar cells keeping the hole recombination as low as possible. Several groups have been working on TiO_2 thin films for surface passivation of c-Si. However, due to several deposition techniques and different chemical precursors the reported results in the literature are quite scattered, as it can be seen in table 2.2.

Si doping type	Si resistivity (Ωcm)	TiO$_2$ deposition method	TiO$_2$ precursor	TiO$_2$ deposition temperature (ºC)	TiO$_2$ layer thickness (nm)	Reference
n-type	3	ALD	TTIP	230	5.5	[8]
p-type	1	ALD	TDMAT	150/200	1.5	[9]
p-type	10	ALD	TDMAT	150	1.5	[9]

Table 2.2: TiO$_2$ deposition examples

3. Methodology / project development:

3.1. ALD

The ALD (Atomic Layer Deposition) is different from other deposition techniques as PVD (Physical Vapor Deposition) or CVD (Chemical Vapor Deposition) because the reactions of the precursors take place on the silicon surface one at a time, as opposed to the other techniques that make the reactions between the precursors and then the result of the reaction is deposited on the silicon. Also the ALD technique can accurately control the thickness of the deposition, because for each cycle only deposits one molecule thickness film.

Al(CH$_3$)$_3$(g)   Al(CH$_3$)$_2$(s)   H$_2$O (g)   Al$_2$O$_3$(s)
Pulse   Purge   Pulse   Purge

Repeat ALD cycle N times

Figure 3.1: ALD process

In the upper image we have an example of ALD process, in this case for Al$_2$O$_3$. Firstly, a pulse of a gas reactive (Al(CH$_3$)$_3$) is introduced into the reaction chamber and then we must wait some time for the material surface to adsorb the reactive. Then a flow of inert gas (N$_2$) is introduced to remove any excess of the reactive. After this, a second gas pulse is activated but this time of another precursor (H$_2$O) which reacts with the first one to create another layer on the surface (Al$_2$O$_3$). Then the reaction chamber is cleared again using a flow of inert gas and the cycle starts again. An example of Al$_2$O$_3$ deposition parameters can be seen in table 4.1.

3.2. Al$_2$O$_3$

3.2.1. Thickness measurement

For thickness measurements we have used ellipsometer. This technique can be used only for polished wafers, because it is based on the polarization change of the reflected light on the wafer.

In our case, we use a 632 nm continuous laser that is polarized. The laser beam is partially reflected by the Al$_2$O$_3$ while most of it goes through the dielectric, which is transparent to this wavelength, up to the c-Si surface where it is again partially reflected. All the reflected light is guided to an analyser that gets the new polarization of the light. The change between the initial polarization and the final one is used to automatically calculate the thickness of the transparent thin film on the c-Si surface.

3.2.2. Lifetime measurement

The instrument to carry out this measurement is a Sinton WCT-120.

The Sinton WCT-120 photoconductance instrument is developed by Sinton Instruments, originally established as Sinton Consulting in 1992, a company dedicated to developing and applying new tools and analysis to R&D and manufacturing in silicon solar cells and integrated circuits [10].

This instrument obtains the effective lifetime (τ_{eff}) as a function of the average minority carrier density (Δn). The parameter τ_{eff} can be considered as the average time of the minority carriers between their generation and their recombination. Then, τ_{eff} takes into account all the recombination processes in the c-Si sample. We are interested in the recombination occurring at the c-Si surface, which is described by a surface recombination velocity S_{eff}. This parameter is a figure of merit in c-Si solar cells where the lower this value the better.
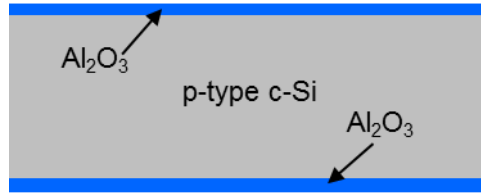

Figure 3.2: Lifetime measurement structure

As it can be seen in figure 3.2, the measured sample is symmetrically coated by Al_2O_3 film. Then, the surface and bulk contributions are combined using the following equation:

$$\frac{1}{\tau_{eff}} = \frac{1}{\tau_{bulk}} + \frac{2S_{eff}}{W} \tag{1}$$

Isolating S_{eff} in equation (1):

$$S_{eff} = \left(\frac{1}{\tau_{eff}} - \frac{1}{\tau_{bulk}} \right) \times \left(\frac{1}{W} \right) \tag{2}$$

where τ_{bulk} and W are the lifetime in the bulk and the thickness of the wafer, respectively.

Since we are using a high quality c-Si, we assume that the only recombination mechanisms in the bulk are the intrinsic ones. In other words, we suppose that τ_{bulk} is only due to τ_{int} that is the intrinsic lifetime of the wafer and can be calculated as [11]:

$$\tau_{int} = \frac{\Delta n}{(np - n_{i,eff}^2)(2.5 \times 10^{-31} g_{eeh} n_0 + 8.5 \times 10^{-32} g_{ehh} p_0 + 3.0 \times 10^{-29} \Delta n^{0.92} + B_{rel} B_{low})} \tag{3}$$

where:

-*n* is the electron density.

-*p* is the hole density.

-*n$_0$* is the thermal equilibrium electron density.

-*p$_0$* is the thermal equilibrium hole density.

-*Δn* is the excess carrier density.

-*n$_i$* is the intrinsic carrier concentration for lowly doped and lowly injected silicon, 9.7×10^9 cm^{-3} at 300 K.

-*n$_{i,eff}$* is the effective intrinsic carrier concentration, according to $n_{i,eff} = n_i e^{\beta \Delta E_g / 2}$.

-*B$_{low}$* is the radiative recombination coefficient for lowly doped and lowly injected silicon, 4.7×10^{-15} cm^3 s^{-1} at 300K.

-*B$_{rel}$* is the relative radiative recombination coefficient.

All S$_{eff}$ calculation are done at *Δn* equal to 10^{15} cm^{-3}, which is a typical value for solar cell operation.

3.2.3. Capacitance-Voltage measurement

The instrument use to obtain this characteristic is a Hewlett Packard 4294A, which is a RF impedance analyser.
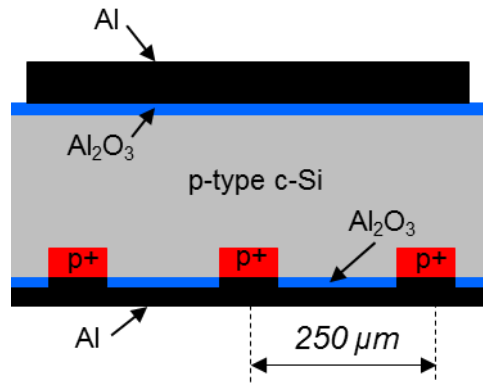

Figure 3.3: C-V measurement structure

As it can be seen in figure 3.3, we deposit an aluminium back contact and dots of different size using a shadow mask on the front side. To metalize the sample, we use a PVD with an electron beam and we deposit around 1 micron of aluminium on both cases. When we have the aluminium deposited, we process the back contact with a laser to create contacts through the dielectric homogeneously distributed. A picture of the front and rear side of one of these sample can be seen in figure 3.4.
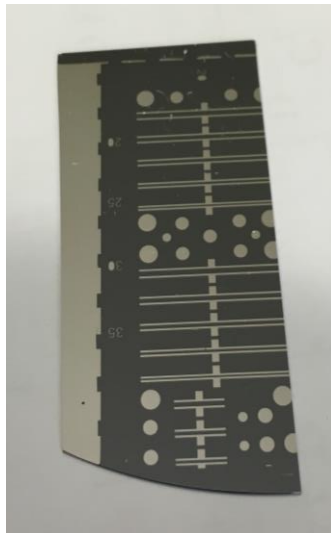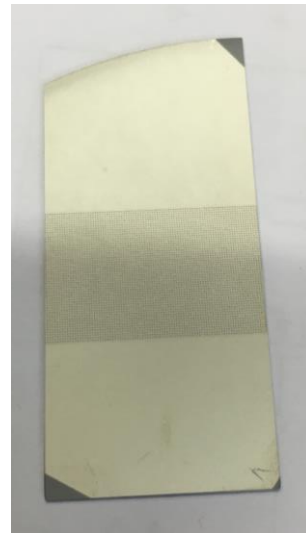
(a) Front side   (b) Rear side

Figure 3.4: Sample to measure C-V

To obtain the Capacitance-Voltage (C-V) characteristic from a sample we make a measure at 1 MHz and sweeping the bias voltage, using a C_sR_s model (capacitor in series with resistor). These measurements can be accurately modelled by classical Metal Insulator Semiconductor (MIS) theory [12]. In this model, we have two free parameters. On the one hand, the equivalent fixed charge density (Q_f) located at the dielectric/c-Si interface. This fix charge helps in the surface passivation, since it repeals one type of carriers reducing the surface recombination rate. On the other hand, a constant interface state density (D_{it}) which models the dangling bonds at the interface. These dangling bonds create states at the energy gap increasing the recombination, since carriers can used them as intermediate steps.

To increase the accuracy of the obtained data, for every sample we take measurements of three different spot sizes. In principle, the relation between the measurement capacitance values is the same than the one for the spot area.

3.3. <u>TiO$_2$</u>

3.3.1. Thickness measurement

This process is equal to the described in chapter 3.2.1.

3.3.2. Lifetime measurement

This process is equal to the described in chapter 3.2.2.

3.3.3. I-V measurement

As in the C-V measurement of Al$_2$O$_3$, before TiO$_2$ deposition in the ALD we have to create a back contact to the n-type c-Si wafer. In this case, the contact is based on a phosphorus doped silicon carbide (SiC$_x$) film which is laser processed in order to create n+ regions inside the c-Si wafer. Next, a titanium/aluminium (Ti/Al) metallization is carried out. Notice that for the TiO$_2$ samples we process the wafer with the laser before contact deposition, in contrast to the Al$_2$O$_3$ where the laser stage takes place after aluminium deposition. On the front side, we define Ti/Al dots of different sizes through the same shadowing mask that we used for Al$_2$O$_3$ samples. A cross section of the sample is shown in figure 3.5.
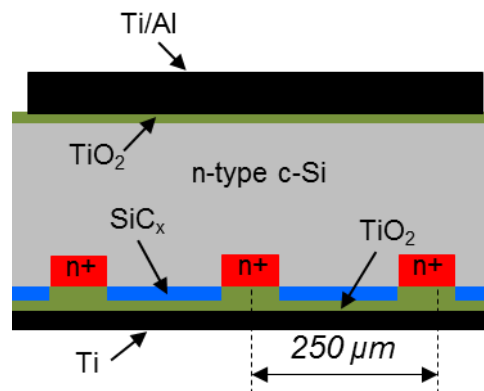

Figure 3.5: I-V measurement structure

When we have all done, we can measure the current-voltage (I-V) with Keithley 2601B and Matlab software developed previously by other thesis student. To do the measurement, we use a 4 wire configuration where we apply current to the device and measure the resulting voltage.

When we have the data of the measurement we have to manipulate it in order to obtain the contact resistance which is the parameter that characterize the quality of the contact.

Firstly, we calculate the total resistance of the sample (R$_{sample}$) by using Ohm's law, in other words, calculating the inverse of the slope of the I-V curve. This resistance has three components: the spreading resistance (R$_{spreading}$) that only depends on the geometry of the spot and the wafer; the back contact resistance (R$_{back\ contact}$), which we consider it negligible, and the last one is the contact resistance (R$_c$), which is what we want to know.

For the spreading resistance, we use the following expression [13]:

$$R_{spreading} = \frac{\rho}{2\pi r} \arctan\left(\frac{2W}{r}\right)$$

(4)

where ρ is the substrate resistivity, W is the wafer thickness and r is the radius of the circular dot. This value can be subtracted from the total measured resistance to obtain the contact resistance. Finally, we multiply R_c by the area of the dot to obtain the specific contact resistance (ρ_c). In principle, this last parameter only depends on the contact quality and must be equal for all dot sizes. The next equation summarizes the process to calculate ρ_c from the measured total resistance of the sample.

$$\rho_C = R_C \cdot A = \left(R_{sample} - R_{spreading}\right) A$$

(5)

4. <u>Results</u>

4.1. <u>Results for Al_2O_3</u>

All the deposits were made with the following parameters per cycle:

$Al(CH_3)_3$ pulse	50 ms
N_2 purge	5 s
H_2O pulse	15 ms
N_2 purge	5 s

Table 4.1: Deposit parameters for Al_2O_3

And for all samples the aluminium oxide was deposited at 200 ºC. An annealing at 400 ºC for 10 minutes was carried out after film deposition to activate the fixed charge density in the film.

4.1.1. Thickness

For the thickness tests, all the samples were cleaned with RCA1+HF1+RCA2, this means:

-RCA1: 1500 ml desionized water (H_2O) + 250 ml hydrogen peroxide (H_2O_2) + 250 ml ammonia solution (NH_3), at 75 ºC for 20 minutes.

-HF1: hydrofluoric acid (HF) in a 1% for 1 minute.

-RCA2: 1500 ml desionized water (H_2O) + 250 ml hydrogen peroxide (H_2O_2) + 250 ml hydrochloric acid (HCl), at 75 ºC for 20 minutes.

We decided not to do HF2 (that is the same that HF1 but after RCA2) because we observed that does not improve significantly the lifetime and for the texturized samples their passivation was degraded after this chemical step.

For the study we have used three types of wafers: n-type polished, p-type polished and n-type with random pyramids surface. This surface texturization is widely used in c-Si solar cells to reduce their front reflectance. To texturize the surface, we use an anisotropic etching to the c-Si with a solution of tetramethylammonium hydroxide (TMAH). This chemical etching has different etching rates depending on c-Si crystal orientation creating random pyramids along the surface. In figure 4.1, a scanning electron microscope (SEM) image of a typical c-Si texturized surface can be seen.
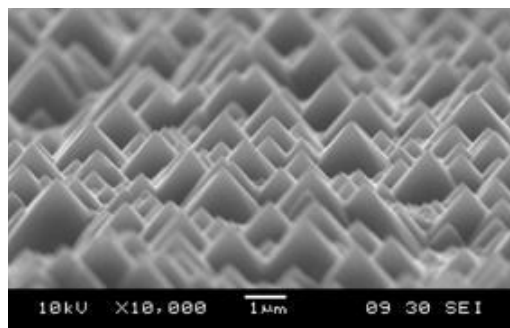

Figure 4.1: Picture of pyramidal texturized surface using TMAH

With the polished wafers, n-type and p-type, we have studied 1, 2, 5, 10, 20 and 50 nm and with the texturized wafers 2, 5, 10, 20 and 50 nm.

4.1.1.1. Surface passivation

In the figure 4.2 and figure 4.3 we can see the obtained effective surface recombination velocity (S_{eff}) values for different Al_2O_3 film thicknesses on both type of substrates. We can see that when the thickness increases S_{eff} decreases until it saturates for thicknesses beyond 10 nm (notice the log scate in the y-axis). From this result, we can say that a minimum Al_2O_3 thickness of 10 nm is necessary to get S_{eff} below 10 cm/s. This result fulfils the milestone M2.1 as it was defined at the beginning of the project.
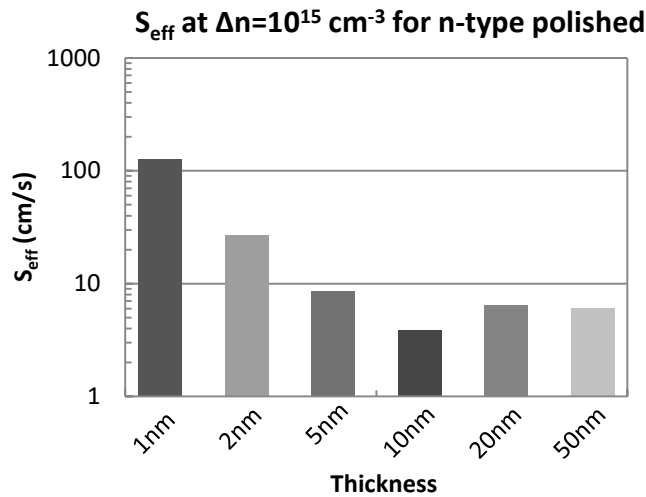

Figure 4.2: S_{eff} as a function of the thickness for Al_2O_3 on n-type polished wafers at $\Delta n=10^{15}\,cm^{-3}$
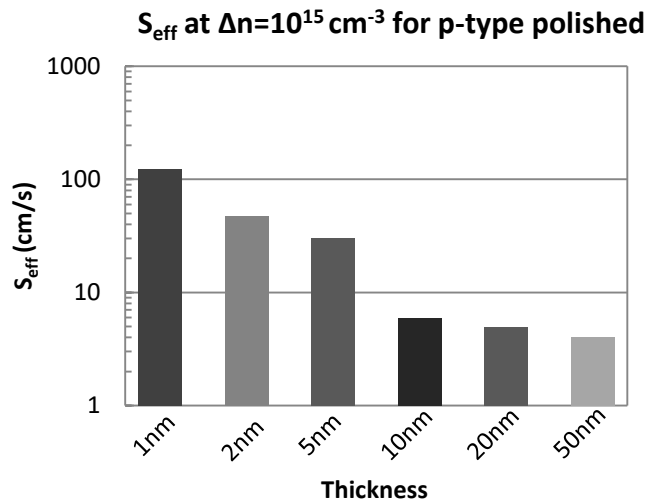

Figure 4.3: S_{eff} as a function of the thickness for Al_2O_3 on p-type polished wafers at $\Delta n=10^{15}\,cm^{-3}$

4.1.1.2. C-V

We only use the p-type samples to measure the C-V due to their easiness to create the rear contact through laser processing. In figure 4.4 we show the measured curves for Al_2O_3 films of 10 and 20 nm. In addition, the best fit with the theoretical model is also shown (solid line).
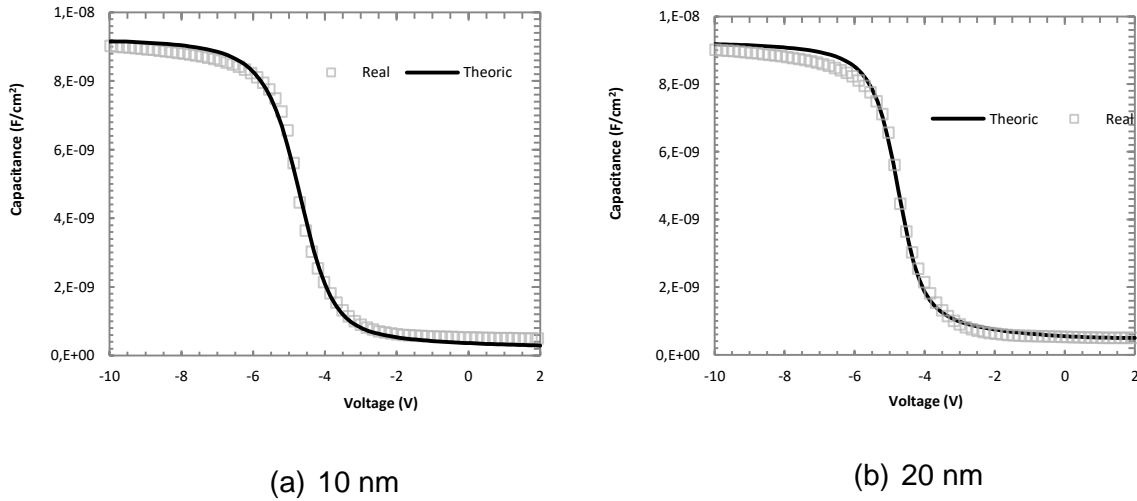

(a) 10 nm

(b) 20 nm

Figure 4.4: C-V results for polished p-type Al_2O_3 samples

From the fitting of the measured curves, we obtain the following values for the fixed charge density at the interface (Q_f) and the interface state density (D_{it}).

	Q_f (cm^{-2})	Dit (cm^{-2} eV^{-1})
10 nm	3.00×10^{12}	4.00×10^{13}
20 nm	5.25×10^{12}	1.30×10^{13}

Table 4.2: Al_2O_3 fixed charge density and interface state density for 10 and 20 nm samples

As it can be seen, the values of Q_f are positive and in the range of 10^{12} cm^{-2}. This result is in complete disagreement with the reported values of Q_f in the literature where only negative values can be found [1]. In addition, the D_{it} value are in the range of 10^{13} cm^{-2}eV^{-1} which is much higher than expected. These results indicate that the interface has an unexpected configuration. Surprisingly, the quality of the surface passivation is excellent with S_{eff} below 10 cm/s. In order to be sure that these results were not an artefact of a particular deposition or in the measurement procedure, we repeated the samples with similar results. A research focusing on this contradiction is currently underway.

4.1.2. Cleaning process

For this study we only have used n-type texturized wafers because is the type of sample where we can notice better the differences between the cleaning processes. Due to the time limitations we have only measured the lifetime of the samples and not the C-V characteristic.

|	Only HF	SOFT$_C$	SOFT$_B$	SOFT$_A$	RCA1	RCA1/2
Reactive proportion	-	1900 ml H$_2$O 50 ml H$_2$O$_2$ 50 ml NH$_3$	1800 ml H$_2$O 100 ml H$_2$O$_2$ 100 ml NH$_3$	1600 ml H$_2$O 200 ml H$_2$O$_2$ 200 ml NH$_3$	1500 ml H$_2$O 250 ml H$_2$O$_2$ 250 ml NH$_3$	1500 ml H$_2$O 250 ml H$_2$O$_2$ 250 ml NH$_3$ ------------------------ 1500 ml H$_2$O 250 ml H$_2$O$_2$ 250 ml HCl
Reactive temperature	-	45 ºC	45 ºC	45 ºC	75 ºC	75 ºC
Reactive time	-	20 minutes	20 minutes	20 minutes	20 minutes	20 minutes
HF1 proportion	1%	1%	1%	1%	1%	1%
HF1 time	1'	1'	1'	1'	1'	1'

Table 4.3: Cleaning processes used

As you can observe in the table we had done six different cleaning processes. They are ordered from the left to the right in function of its theoretical aggressiveness.

With these tests, we want to find the better agreement between the aggressiveness and the passivation results, and also the consumption of reactive.

We started with only HF, RCA1 and SOFT$_A$ cleanings and we notice that we obtained bad results that do not match with previous experiments. Then, we decided to make a HF in a 1% for 1 minute prior to any cleaning to try if the results improve, after that we made the SOFT$_B$ cleaning using this new procedure. We obtained that SOFT$_B$ cleaning gave us better results than RCA1 and SOFT$_A$, which indicates that the RCA1 and SOFT$_A$ cleanings were not made correctly. For this reason, we think that when you texturize a wafer and leave it for a long time, in our case 1 month approximately, an oxide layer appears on the surface, and this oxide is not well removed with the cleaning and we need to make a previous HF to remove it.

After reaching this conclusion, we made all the cleaning processes with a previous HF and we saw that the results have the tendency that we expected as show the figure 4.5. For more aggressiveness lower Seff and better passivation, but all the SOFT$_X$ cleanings give us similar results than a normal cleaning process, but with less aggressiveness which means that destroy less material on the surface. This result is quite good because for some processes during the solar cell development we need to clean the surface of the samples, but trying not to etch previous layers that were already deposited onto the c-Si surface.
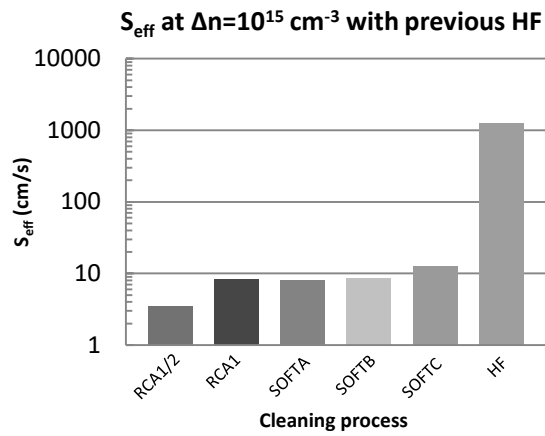
(a) Cleaning processes with previous HF
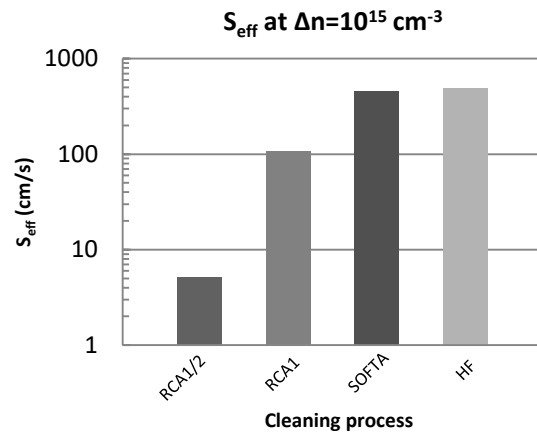
(b) Cleaning processes without previous HF

Figure 4.5: S_{eff} as a function of the cleaning process for Al_2O_3 on n-type texturized wafers at $\Delta n=10^{15}$ cm^{-3}

4.2. Results for TiO$_2$

All the deposits were made with the following parameters per cycle:

TDMAT pulse	100 ms
N$_2$ purge	10 s
H$_2$O pulse	15 ms
N$_2$ purge	10 s

Table 4.4: Deposit parameters for TiO$_2$

4.2.1. Thickness

For the thickness tests all the samples were cleaned with RCA1+HF1+RCA2+HF2, this means:

-RCA1: 1500 ml desionized water (H$_2$O) + 250 ml hydrogen peroxide (H$_2$O$_2$) + 250 ml ammonia solution (NH$_3$), at 75 ºC for 20 minutes.

-HF1: hydrofluoric acid (HF) in a 1% for 1 minute.

-RCA2: 1500 ml desionized water (H$_2$O) + 250 ml hydrogen peroxide (H$_2$O$_2$) + 250 ml hydrochloric acid (HCl), at 75 ºC for 20 minutes.

-HF2: hydrofluoric acid (HF) in a 1% for 1 minute.

And for all samples the titanium oxide was deposited at 125 ºC despite that at lower temperatures we obtain better results, because the ALD is usually at this temperature and we need so much time to go to lower values.

For this study we only have used n-type polished wafers, and we have studied the thickness of 10, 15, 30 and 60 cycles which means approximately 0.6, 0.9, 1.8 and 3.6 nm.

For all the polished samples, we have introduced another one with silicon carbide (SiC$_x$) on the rear face to make the I-V measurements.

4.2.1.1. Surface passivation

From the figure 4.6 where the S_{eff} values for different thicknesses are shown, we can conclude that from 1.8 nm to lower thicknesses the effective recombination velocity saturates. As opposite with the Al_2O_3, with the TiO_2 when you reduce the thickness the S_{eff} is improved.
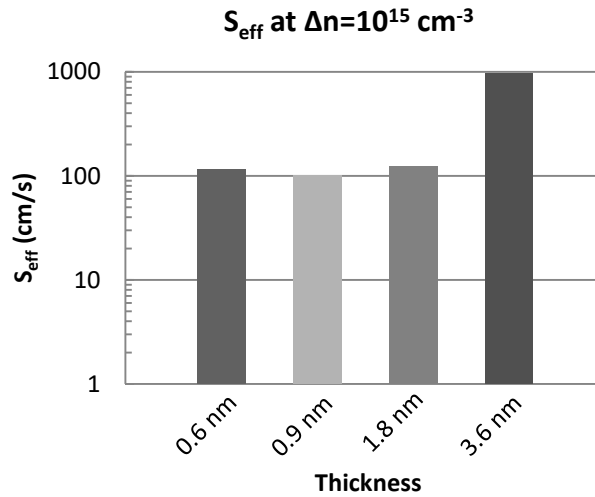

Figure 4.6: S_{eff} as a function of the thickness for TiO_2 on n-type polished wafers at $\Delta n=10^{15}\ cm^{-3}$

These results are from 1 week after deposit the dielectric layer (TiO_2), because with this material we need to wait to stabilize the surface passivation. In figure 4.7 is showed the S_{eff} of the 1.8 nm sample just after deposition, one day after and one week after. Further research is needed to understand this behaviour.
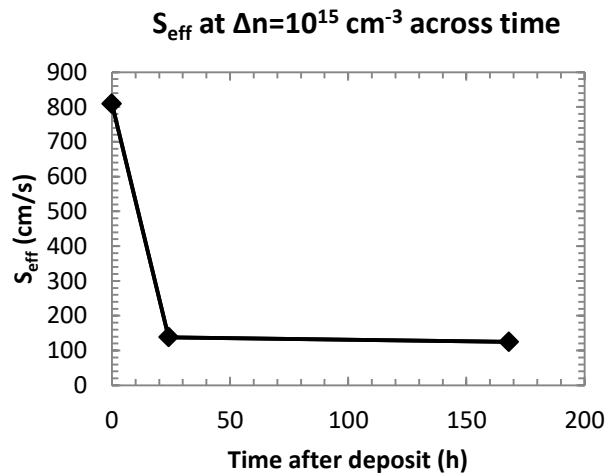

Figure 4.7: S_{eff} of 1.8 nm sample in function of time after TiO_2 deposit at $\Delta n=10^{15}\ cm^{-3}$

4.2.1.2. I-V

In order to know how affects the thickness of the TiO_2 layer to the contact resistivity we measure the I-V characteristic curve as explained in section 3.3.3 and the results are showed in figure 4.8.
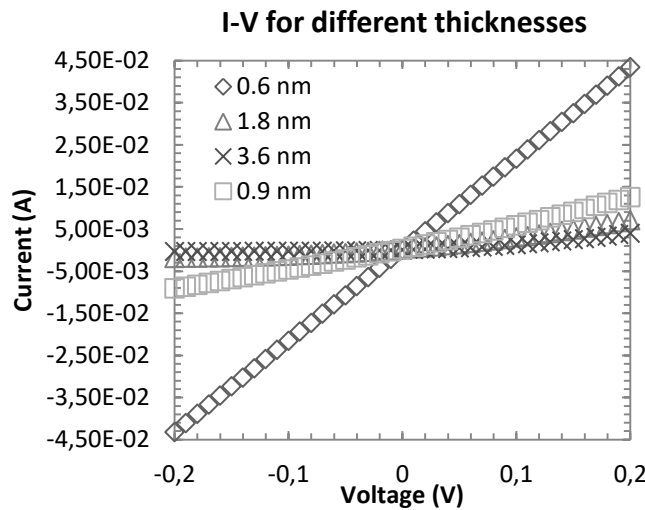

Figure 4.8: I-V of TiO_2 samples for different thicknesses

In the previous figure, we have plot the I-V curves for the four different thicknesses studied only for the big spot for a direct comparison. As it can be seen, TiO_2 layers thicker than 1.8 nm results in non-linear I-V curves indicating a non-ohmic contact. For the sample of 0.9 nm a linear trend is observed and for 0.6 nm the resistance is decreased resulting in higher currents, i.e. lower resistance. Focusing on these last samples, we measure the I-V characteristic for the three dot sizes. The obtained curves are shown in figure 4.9.
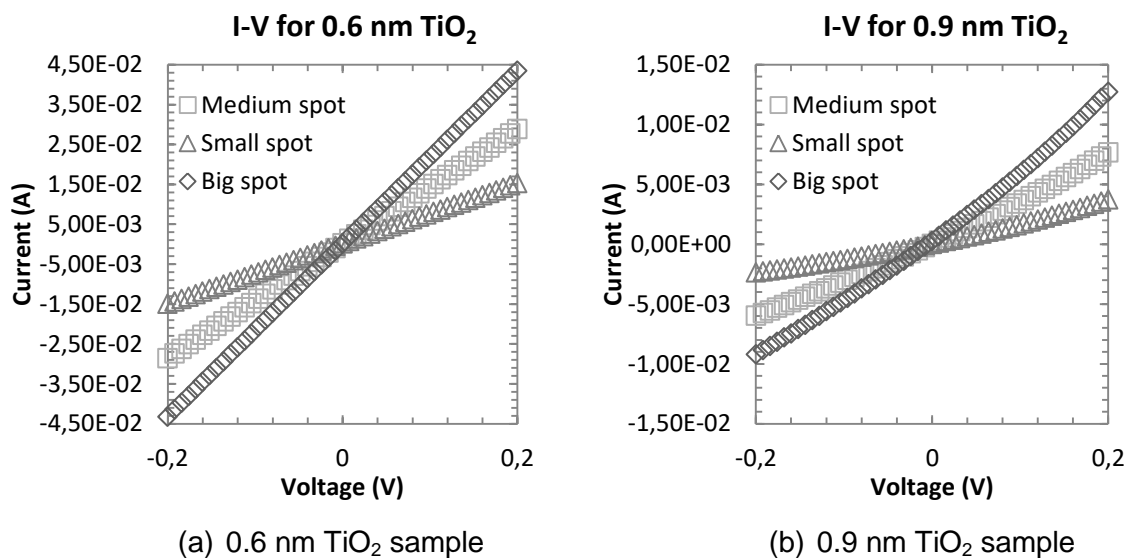
(a) 0.6 nm TiO_2 sample

(b) 0.9 nm TiO_2 sample

Figure 4.9: I-V results for TiO_2 samples with different spot sizes

Following the procedure described in methodology section 3.3.3, we calculate the specific contact resistance ρ_c.

0.9 nm sample				
Spot	$R_{Sample}(\Omega)$	$R_{spreading}(\Omega)$	$R_C(\Omega)$	$\rho_C(m\Omega \cdot cm2)$
Big	18,52	2,00	16,52	518,99
Medium	29,67	3,35	26,32	465,11
Small	69,00	6,62	62,38	489,93

0.6 nm sample				
Spot	$R_{Sample}(\Omega)$	$R_{spreading}(\Omega)$	$R_C(\Omega)$	$\rho_C(m\Omega \cdot cm^2)$
Big	4,62	2,00	2,62	82,31
Medium	6,97	3,35	3,62	63,97
Small	13,23	6,62	6,61	51,91

Table 4.5: Contact resistivity calculation for 0.6 and 0.9 nm samples

As it can be seen, for the 0.9 nm sample similar values for ρ_c are obtained for all dot sizes in the range of 450-550 $m\Omega \cdot cm^2$. The quality of this contact is not enough to be applied to high-efficiency solar cells. On the other hand, the 0.6 nm sample shows better results, despite some scattering with the size, with ρ_c in the range of 50-100 $m\Omega \cdot cm^2$. These values combined to the obtained S_{eff} values in the range of 100 cm/s fulfil the milestone defined in table 1.5. Additionally, this thin TiO_2 layer is a promising candidate to be used in high-efficiency c-Si solar cells.

4.2.2. Temperature

In the temperature study we want to see the effect of the deposition temperature on the samples characteristics. Due to lack of time, we could not measure the I-V behaviour, for this reason we only have the surface passivation results.

In this study, as in the previous one, we have used only n-type polished wafers with TiO_2 layers of 0.9 nm. The temperatures studied are: 85, 125 and 175 ºC. Lower temperatures are not available in the ALD tool.

The figure 4.10 shows that when the temperature increases the S_{eff} increases too. Then, for surface passivation based on TiO_2, it is better to deposit at low temperature. This result is interesting for solar cell fabrication, since high temperature processes can degrade the performance of certain materials and/or interfaces already present in the device.
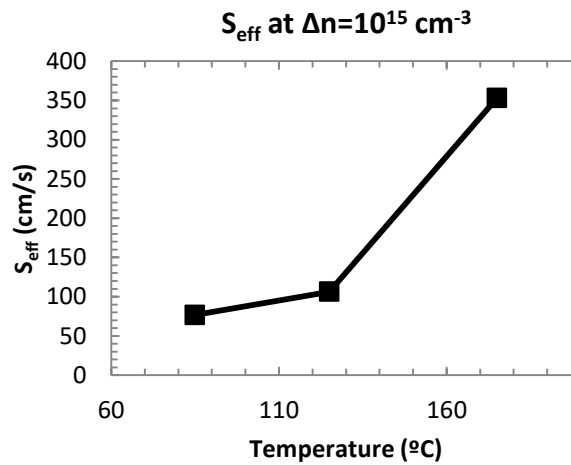

Figure 4.10: S_{eff} of TiO_2 15 cycles samples in function of temperature at $\Delta n=10^{15}$ cm^{-3}

5. <u>Budget</u>

Component	Quantity	Cost (€)	Total cost (€)
Wafer	8	23.00	184.00
Chemical reactives: H_2O_2, HCl, HF, NH_3	15 liters	10.00 €	150.00
Personal	720 h	8.00	5,760.00
Total	-	-	**6,094.00**

Table 5.1: Budget

6.   <u>Conclusions and future development:</u>

The Al_2O_3 has the expected surface recombination velocity results, those are similar to the results that we can find in the literature with S_{eff} below 10 cm/s. We have obtained a minimum thickness to get this surface passivation of 10 nm. However, from the C-V measurements we have deduced a positive charge density at the interface instead of negative one, which is typically reported in the literature. In addition, we obtain higher interface state density values than expected. In addition, from the study focused on different cleanings, we can conclude that softer cleanings can be carried out with similar results in surface passivation. This is an important result since it can help to the compatibility of these chemical steps in the solar cell fabrication processes.

Regarding TiO_2 films, we have achieved good results in specific contact resistance in the range 75 m$\Omega \cdot$cm^2 range with TiO_2 films well below 1 nm. This result combined to the surface passivation obtained (S_{eff} in the range of 100 cm/s) indicate a high potential of these films to be included in c-Si high-efficiency solar cells.

Apart from these conclusions, some future work to do is the following items:

- Clarify the origin of the charge with Al_2O_3.

- Improve the TiO_2 recipe in order to get lower ρ_c.

- Extend the temperature study of TiO_2 films and measure its I-V.

- Do thick TiO_2 deposition to be able to accurately measure its thickness.

Bibliography:

[1] B. Hoex, J. J. H. Gielis, M. C. M. van de Sanden, and W. M. M. Kessels, J. Appl. Phys. 104, 113703 (2008)

[2] G. S. Higashi and C. G. Fleming, Appl. Phys. Lett. 55, 1963 (1989).

[3] D. G. Park, H. J. Cho, K. Y. Lim, C. Lim, I. S. Yeo, J. S. Roh, and J. W. Park, J. Appl. Phys. 89, 6275 (2001).

[4] I. S. Jeon, J. Park, D. Eom, C. S. Hwang, H. J. Kim, C. J. Park, H. Y. Cho, J. H. Lee, N. I. Lee, and H. K. Kang, Jpn. J. Appl. Phys., Part 1 42, 1222 (2003).

[5] I. Martín, P. Ortega, M. Colina, A. Orpella, G. López, R. Alcubilla, Progr. Photov.: Res. Appl., 21, 1171 (2012).

[6] P. Ortega, I. Martín, G. López, M. Colina, A. Orpella, R. Alcubilla, Solar Energy Materials and Solar Cells, 106, 80 (2012).

[7] G. López, P. Ortega, C. Voz, I. Martín, M. Colina, A. Morales-Vilches, A. Orpella, R. Alcubilla, Beilstein Journal of Nanotechonology, 4, 726 (2013).

[8] X. Yang and K. Weber, in Proc. IEEE 42nd Photovoltaic Spec. Conf., 2015, pp. 1–4.

[9] Karim Mohamed Gad, Daniel V¨ossing, Armin Richter, Bruce Rayner, Leonhard M. Reindl, Suzanne E. Mohney, and Martin Kasemann, IEEE Journal of Photovoltaics, 6, 649 (2016).

[10] Sinton Consultin Inc.url: http:// www.sintoninstruments.com/index.html/.

[11] A. Richter, S.W. Glunz, F. Werner, J. Schmidt, A. Cuevas, Physical Review B 86: 165202 (2012).

[12] E.H. Nicollian and J.R. Brewster, "MOS (Metal Oxide Semiconductor) Physics and Technology", Ed. Wiley (2002).

[13] R.H. Cox, H. Strack, Sol. State El. 10, 1213 (1967).

Glossary

A
Al: Aluminium
Al_2O_3: Aluminium Oxide
$Al(CH_3)_3$: Trimethylaluminium
ALD: Atomic Layer Deposition
C
c-Si: Crystalline Silicon
C-V: Capacitance-Voltage
CVD: Chemical Vapour Deposition
D
D_{it}: Interface State Density
Δn: Minority Carrier Density
H
HCl: Hydrochloric Acid
H_2O: Water
H_2O_2: Hydrogen Peroxide
HF: Hydrofluoric Acid
I
I-V: Current-Voltage
ICFO: Institut de Ciències Fotòniques
M
MIS: Metal Insulator Semiconductor
MNT: Micro and Nano Technologies

N
N_2: Nitrogen
NH_3: Ammonia
P
PVD: Physical Vapour Deposition
Q
Q_f: Fixed Charge Density
R
R&D: Research & Development
RF: Radio Frequency
S
S_{eff}: Effective Surface Recombination Velocity
SEM: Scanning Electron Microscope
SiC_x: Silicon Carbide
T
Ti: Titanium
TiO_2: Titanium Dioxide
TMAH: Tetramethylammonium hydroxide
τ_{eff}: Effective Lifetime
U
UPC: Universitat Politècnica de Catalunya